Supporting Information

New honeycomb MOF for C_2H_4 purification and C_3H_6 enrichment by separating methanol to olefin products

Lin Zhang,[a] Li-Na Ma,[a] Gang-Ding Wang,[a] Lei Hou,*[,a] Zhonghua Zhu[b] and Yao-Yu Wang*[,a]

[a]*Key Laboratory of Synthetic and Natural Functional Molecule of the Ministry of Education, Xi'an Key Laboratory of Functional Supramolecular Structure and Materials, College of Chemistry & Materials Science, Northwest University. Xi'an, 710069, P. R. China.*

[b]*School of Chemical Engineering, The University of Queensland Brisbane 4072, Australia.*

**To whom correspondence should be addressed. E-mail: lhou2009@nwu.edu.cn (Lei Hou); wyaoyu@nwu.edu.cn (Yao-Yu Wang).*

X-ray crystallographic measurements

The single crystal diffraction data was conducted at 296(2) K on a Bruker SMART APEX II CCD detector diffractometer. The structure was solved by direct method and refined on F^2 by full-matrix least-squares procedures with SHELXL-2014 software package. The non-hydrogen atoms were refined anisotropically, while the hydrogen atoms added to their geometrically ideal positions and were refined isotropically. For the disordered lattice molecules that cannot be well refined, the SQUEESE procedure was adopted in structural refinement. The results of structure refinement and selected bond distances/angles are listed in Tables S1 and S2, respectively.

Calculation of sorption heat using Virial 2 model

$$\ln P = \ln N + 1/T\sum_{i=0}^{m} a_i N^i + \sum_{i=0}^{n} b_i N^i \qquad\qquad Q_{\mathrm{st}} = -R\sum_{i=0}^{m} a_i N^i$$

The above virial expression was used to fit the combined isotherm data (measured at 273 and 298 K) for Mn-dtzip, where P is the pressure, N is the adsorbed amount, T is the temperature, a_i and b_i are virial coefficients, and m and N are the number of coefficients used to describe the isotherms. Q_{st} is the coverage-dependent enthalpy of adsorption and R is the universal gas constant.

IAST adsorption selectivity calculation

The experimental isotherm data for pure C_2H_4 and C_3H_6 (measured at 273 and 298 K) was fitted using a double-site Langmuir-Freundlich (DSLF) model:

$$N = A_1\frac{b_1P^{c_1}}{1+b_1P^{c_1}} + A_2\frac{b_2P^{c_2}}{1+b_2P^{c_2}}$$

Where A and p are the adsorbed amounts and the pressure of component i, respectively.

The adsorption selectivity for binary mixtures defined by

$$S_{i/j} = \frac{x_i * y_j}{x_j / y_i}$$

was calculated using the Ideal Adsorption Solution Theory (IAST) of Myers and Prausnitz. Where x_i is the mole fraction of component i in the adsorbed phase and y_i is the mole fraction of component i in the bulk.

The separation potential (Δq)

For screening MOFs for separation of binary mixtures of components 1 and 2, the adsorption selectivity, S_{ads}, is defined by

$$S_{ads} = \frac{q_1/q_2}{y_{10}/y_{20}}$$

In eq, y_{10} and y_{20} are the mole fractions of the bulk gas phase mixture. The $C_3H_6(1)/C_2H_4(2)$ mixture separations are envisaged to be carried out in fixed bed adsorbents. In such devices, the separations are dictated by a combination of adsorption selectivity and uptake capacity. Using the shock wave model for fixed bed adsorbents, Krishna[1, 2] has suggested that the appropriate metric is the separation potential, Δq_1. The appropriate expression describing the productivity of pure C_3H_6 in the desorption phase of fixed-bed operations is

$$\Delta q_1 = q_1 - q_2 \frac{y_{10}}{y_{20}}$$

In eq, y_{10} and y_{20} are the mole fractions of the feed mixture during the adsorption cycle. In the derivation of eq, it is assumed that the concentration "fronts" traversed the column in the form of shock waves during the desorption cycle. The molar loadings q_1 and q_2 of the two components are determined using the Ideal Adsorbed Solution Theory (IAST) of Myers and

Prausnitz using the unary isotherm fits as data inputs.[3] The physical significance of Δq_1 is the maximum productivity of pure C_3H_6(1) that is achievable in PSA operations.

GCMC simulation

Grand canonical Monte Carlo (GCMC) simulations were performed for the gas adsorption in the framework by the Sorption module of Material Studio (Accelrys. Materials Studio Getting Started). The partial charges for atoms of the framework were derived from QEq method and QEq neutral 1.0 parameter. One unit cell was used during the simulations. The interaction energies between the gas molecules and framework were computed through the Coulomb and Lennard-Jones 6-12 (LJ) potentials. All parameters for the atoms were modeled with the universal force field (UFF) embedded in the MS modeling package. A cutoff distance of 12.5 Å was used for LJ interactions, and the Coulombic interactions were calculated by using Ewald summation. For each run, the 3×10^6 maximum loading steps, 3×10^6 production steps were employed.

Breakthrough Experiments

The breakthrough experiment was performed on the Quantachrome dynaSorb BT equipments at 298/273 K and 1 atm (Ar as the carrier gas). The activated Mn-dtzip (1.012 g) was filled into a packed column of 4.2×80 mm, and then the packed column was washed with Ar at a rate of 7 mL min^{-1} at 343 K for 60 minutes to further activate the samples. Between two breakthrough experiments, the adsorbent was regenerated by Ar flow of 7 mL min^{-1} for 35 min at 353 K to guarantee a complete removal of the adsorbed gases.

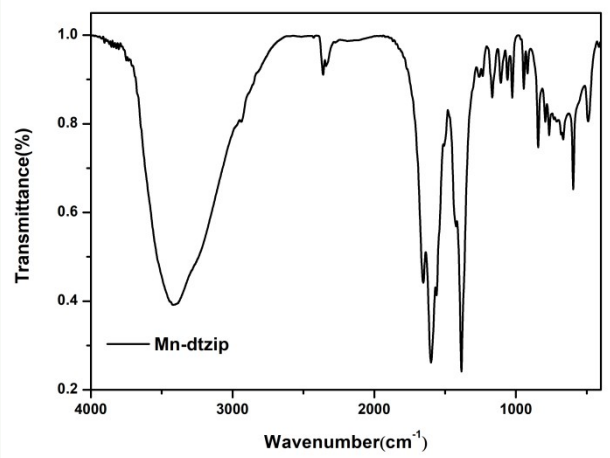

Fig. S1. FTIR spectra of Mn-dtzip.

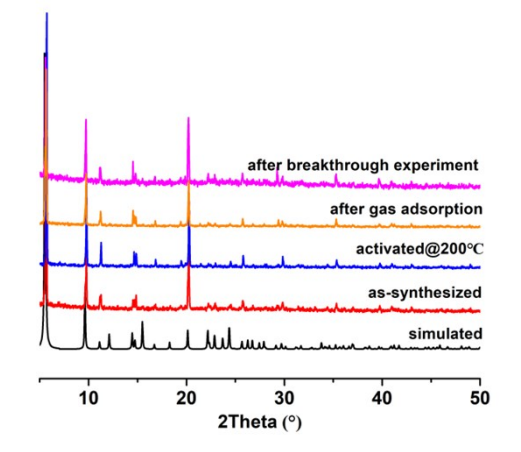

Fig. S2. PXRD patterns of Mn-dtzip after different treatments.

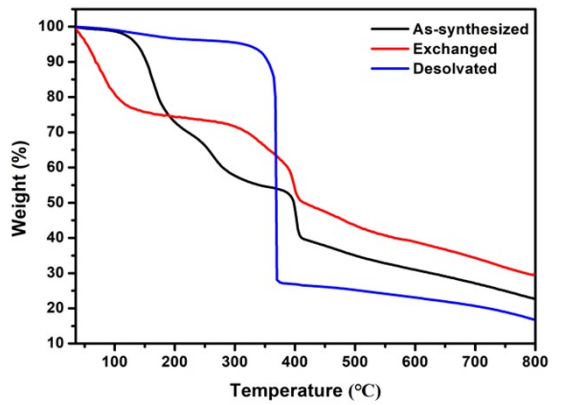

Fig. S3. TGA curves for Mn-dtzip.

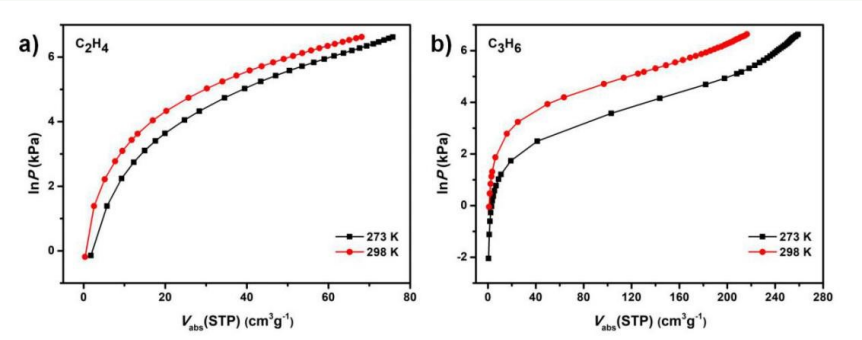

Fig. S4. Adsorption isotherms of Mn-dtzip fitted by Virial 2 model (the fitted parameters were listed in Table S3).

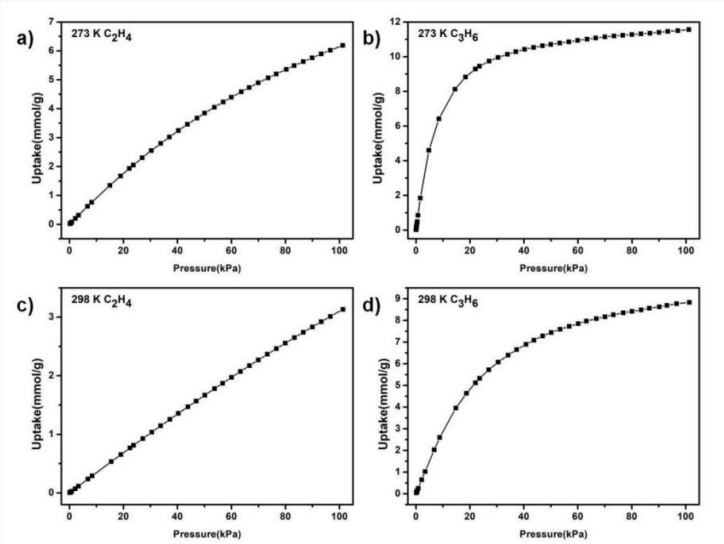

Fig. S5. Gas adsorption isotherms fitting by DSLF model at 273/298 K (the fitted parameters were listed in Table S4).

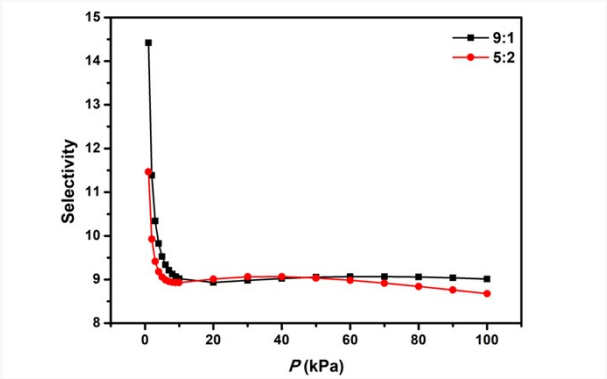

Fig. S6. IAST selectivities for different C_2H_4-C_3H_6 mixtures at 298 K.

Table S1. The details about solvents and chemicals.

Chemicals	Purities	Brands
$MnCl_2 \cdot 4H_2O$	99.0%	aladdin
DMF	99.5%	Greagent
HNO_3	65%	Greagent
H_2dtzip	98.0%	Adamas

Table S2. Crystallographic data of Mn-dtzip.

Empirical formula	$C_8H_8MnN_5O_3$
Formula weight	157(2)
Crystal system	Hexagonal
Space group	$P6_4$
a (Å)	18.3490(3)
b (Å)	18.3490(3)
c (Å)	8.2189(2)
α, β, γ(°)	90, 90, 120
Z, V (Å^3)	6, 2396.45(10)
D_c (g cm^{-3}), μ (mm^{-1})	1.152, 0.829
Reflns collected/unique/	32741 / 2939
R_{int}, GOF	0.0628, 1.182
R_1[a], wR_2[b] [I > 2σ]	0.0308, 0.0755

[a] $R_1 = \Sigma||F_o| - |F_c||)/\Sigma|F_o|$; [b] $wR_2 = [\Sigma w(F_o^2 - F_c^2)^2/\Sigma w(F_o^2)^2]^{1/2}$.

Table S3. Selected bond lengths (Å) and bond angles (°) for Mn-dtzip.

Mn(1)-O(3)	2.139(3)	O(3)-Mn(1)-N(3)#2	97.77(13)
Mn(1)-O(1)	2.210(3)	O(1)-Mn(1)-N(3)#2	81.43(11)
Mn(1)-O(1)#1	2.214(3)	O(1)#1-Mn(1)-N(3)#2	106.37(12)
Mn(1)-N(3)#2	2.216(3)	O(3)-Mn(1)-N(1)	90.11(12)
Mn(1)-N(1)	2.217(3)	O(1)-Mn(1)-N(1)	80.68(10)
Mn(1)-N(2)#3	2.458(3)	O(1)#1-Mn(1)-N(1)	85.21(10)
O(1)-Mn(1)#3	2.214(3)	N(3)#2-Mn(1)-N(1)	160.26(12)
N(2)-Mn(1)#1	2.458(3)	O(3)-Mn(1)-N(2)#3	163.37(11)
N(3)-Mn(1)#5	2.216(3)	O(1)-Mn(1)-N(2)#3	76.37(10)
O(3)-Mn(1)-O(1)	88.68(11)	O(1)#1-Mn(1)-N(2)#3	74.24(10)
O(3)-Mn(1)-O(1)#1	118.85(11)	N(3)#2-Mn(1)-N(2)#3	87.30(11)
O(1)-Mn(1)-O(1)#1	149.09(9)	N(1)-Mn(1)-N(2)#3	80.43(11)

Symmetry transformations used to generate equivalent atoms: #1 -x+y+1, -x+1, z-1/3; #2 -x+y+1, -x+1, z+2/3; #3 -y+1, x-y, z+1/3; #4 -x+1, -y+1, z; #5 -y+1, x-y, z-2/3.

Table S4. Fitting parameters of the adsorption heats for Mn-dtzip.

	C_2H_4	C_3H_6
a0	-2949.18889	-4200.78352
a1	-0.69307	-1.52258
a2	0.02317	0.02901
a3	-1.38843E-4	-1.52035E-4
a4	3.4771E-7	3.77587E-7
b0	12.11093	14.20636
R^2	0.99976	0.99954
Chi^2	8.471E-4	0.0027

Table S5. Fitting parameters of IAST selectivity for Mn-dtzip at 273/298 K.

	273 K C_2H_4	273 K C_3H_6	298 K C_2H_4	298 K C_3H_6
A1	16.3799	41.88179	17.3019	4.78853
b1	0.00566	0.00182	0.00182	0.01395
c1	1.03366	0.5201	1.0397	0.48139
A2	1.19966	11.15715	0.00562	9.54685
b2	-0.00231	0.10506	994.79499	0.02404
c2	1.0069	1.16804	77.02079	1.21342
R^2	1	0.99997	1	0.99999
Chi^2	1.73466E-5	6.6698E-4	3.93865E-6	1.1006E-4

Table S6. IAST selectivity of C_3H_6/C_2H_4 at 1 atm and 298 K for the equimolar binary C_3H_6-C_2H_4 mixtures in different Materials.

Materials	C_3H_6 Uptake ($cm^3\ g^{-1}$)	C_2H_4 Uptake ($cm^3\ g^{-1}$)	Selectivity
ANPC-2-700[1]	203.4	105.1	9.81
Mn-dtzip (This work)	**216.4**	**76.7**	**8.6**
NEM-7-Cu[2]	75.5	29	8.6
MFM-202a[3]	160.8	64.96	8.4
srl-MOF[4]	30.1	21.4	8.09
iso-MOF-4[5]	254.5	73.1	7.74
spe-MOF[4]	236.9	48.9	7.7
iso-MOF-3[5]	234.7	66	7.04
NEM-4[2]	197.4	164.1	6.8
iso-MOF-2[5]	254.1	71.4	6.6
LIFM-38[6]	58	20	6.4
HKUST-1[7]	137.4	102.14	5.8
UPC-33[8]	94.3	31.1	5.7

Yb-**pek**-MOF[9]	127.3	41.7	5.4
iso-MOF-1[5]	209	51	5.1
(Cr)-MIL-101-SO_3Ag[10]	105.84	63.95	4.8
Mg-MOF-74[11]	149.98	161.28	4.7
PCP-1[12]	70.672	56.67	3.6
$[Cd_2(AzDC)_2(TPT)_2](DMF)_3$[13]	59.84	44.95	1.2

Table S7. Breakthrough experiment of Mn-dtzip at different test conditions.

273 K

C_2H_4/C_3H_6/Ar (v/v/v)	Flow rate (mL min^{-1})	C_2H_4 Retention time ($min\ g^{-1}$)	C_3H_6 Retention time ($min\ g^{-1}$)	Δt ($min\ g^{-1}$)	C_2H_4 Collection volume ($cm^3\ g^{-1}$)	C_3H_6 Collection volume ($cm^3\ g^{-1}$)	C_3H_6, recovered from the bed (%)
5/5/90	5	26.4	116.6	90.2	25.9	29.0	90.0
5/2/93	5	26.3	196.0	169.7	44.0	19.6	79.9
9/1/90	5	23.3	236.7	213.4	98.2	11.6	58.4
20/20/60	8	8.9	21.1	12.2	30.6	33.5	91.0
25/10/65	7	9.9	40.6	30.7	65.8	28.1	84.2
36/4/60	8	9.1	62.2	53.1	164.4	19.6	57.0

298 K

C_2H_4/C_3H_6/Ar (v/v/v)	Flow rate (mL min^{-1})	C_2H_4 Retention time ($min\ g^{-1}$)	C_3H_6 Retention time ($min\ g^{-1}$)	Δt ($min\ g^{-1}$)	C_2H_4 Collection volume ($cm^3\ g^{-1}$)	C_3H_6 Collection volume ($cm^3\ g^{-1}$)	C_3H_6 recovered from the bed (%)
5/5/90	5	13.3	78.0	64.7	17.5	19.4	90.6
5/2/93	5	12.8	109.3	96.5	25.3	10.8	84.7
9/1/90	5	14.1	120.5	106.4	47.8	6.0	49.3
20/20/60	8	7.3	18.8	11.5	26.6	29.9	89.8
25/10/65	7	7.5	32.3	24.8	49.2	22.3	75.3
36/4/60	8	5.6	40.7	35.1	109.6	12.8	51.0

Table S8. Breakthrough results of reported materials for C_2H_4/C_3H_6 separation.

Materials	Temperature (K)	Flow rate (mL min^{-1})	Mixture composition and proportion (v/v)	C_3H_6/C_2H_4 approximate retention time difference (min g^{-1})
iso-MOF-4[5]	298	2.67	C_2H_4/C_3H_6 50/50	95
spe-MOF[4]	298	2	C_2H_4/C_3H_6 50/50	67
		4	C_2H_4/C_3H_6 50/20	37
		5	C_2H_4/C_3H_6 90/10	36
this work	298	5	C_2H_4/C_3H_6/Ar 5/5/90	65
		5	C_2H_4/C_3H_6/Ar 5/2/93	97
		5	C_2H_4/C_3H_6/Ar 9/1/90	106
		8	C_2H_4/C_3H_6/Ar 20/20/60	12
		7	C_2H_4/C_3H_6/Ar 25/10/65	25
		8	C_2H_4/C_3H_6/Ar 36/4/60	35
UTSA-35a[14]	296	/	$CH_4/C_2H_2/C_2H_4/C_2H_6/C_3H_6/C_3H_8$ 16.7/16.7/16.7/16.7/16.7/16.7	32
ANPC-2-700[1]	298	/	$CH_4/C_2H_4/C_2H_6/C_3H_6/C_3H_8$/He 5/5/5/5/5/75	35.6
C-600[15]	273	/	C_2H_4/C_3H_6 50/50	4
ZU-16-Co[16]	298	2	$C_2H_2/C_3H_4/C_2H_4/C_3H_6$ 0.5/0.5/49.5/49.5	2

CR-COF-2[17]	298	1	C_2H_4/C_3H_6	35
			50/50	
		2	C_2H_4/C_3H_6	37
			50/20	
		4	C_2H_4/C_3H_6	27
			90/10	
HOF-FJU-1[18]	333	2	$CH_4/C_2H_4/C_2H_6/C_3H_6/C_3H_8/CO_2/H_2$	80
			31/10/25/10/10/1/13	

REFERENCES

1) P. Zhang, X. Wen, L. Wang, Y. Zhong, Y. Su, Y. Zhang, J. Wang, J. Yang, Z. Zeng and S. Deng. *Chem. Eur. J*., 2020, **381**, 122731.

2) X. Liu, C. Hao, J. Li, Y. Wang, Y. Hou, X. Li, L. Zhao, H. Zhu and W. Guo. *Inorg. Chem. Front*., 2018, **5**, 2898-2905.

3) S. Gao, C. G. Morris, Z. Lu, Y. Yan, H. G. W. Godfrey, C. Murray, C. C. Tang, K. M. Thomas, S. Yang and M. Schröder. *Chem. Mater*., 2016, **28**, 2331-2340.

4) H. Fang, B. Zheng, Z.-H. Zhang, H.-X. Li, D.-X. Xue and J. Bai. *Angew. Chem. Int. Ed*., 2021, **60**, 16521-16528.

5) W. Fan, X. Wang, X. Zhang, X. Liu, Y. Wang, Z. Kang, F. Dai, B. Xu, R. Wang and D. Sun. *ACS Central Sci*., 2019, **5**, 1261-1268.

6) C. Chen, Z. Wei, Q. Qiu, Y. Fan, C. Cao, H. Wang, J. Jiang, D. Fenske and C. Su. *Cryst. Growth Des*., 2017, **17**, 1476-1479.

7) W. Su, A. Zhang, Y. Sun, M. Ran and X. Wang. *J. Chem. Eng. Data*., 2017, **62**, 417-421.

8) W. Fan, Y. Wang, Q. Zhang, A. Kirchon, Z. Xiao, L. Zhang, F. Dai, R. Wang and D. Sun. *Chem. Eur. J*., 2018, **24**, 2137-2143.

9) W. Wei, X. Guo, Z. Zhang, Y. Zhang and D. Xue. *Inorg. Chem. Commun*., 2021, **133**, 108896.

10) G. Chang, M. Huang, Y. Su, H. Xing, B. Su, Z. Zhang, Q. Yang, Y. Yang, Q. Ren, Z. Bao and B. Chen. *Chem. Commun*., 2015, **51**, 2859-2862.

11) X. Wu, Z. Bao, B. Yuan, J. Wang, Y. Sun, H. Luo and S. Deng. *Micropor. Mesopor. Mat*., 2013, **180**, 114-122.

12) D. Geng, M. Zhang, X. Hang, W. Xie, Y. Qin, Q. Li, Y. Bi and Z. Zheng. *Dalton Trans*., 2018, **47**, 9008-9013.

13) Y. Zhang, X.-Q. Meng, H.-J. Ding, X. Wang, M.-H. Yu, S.-M. Zhang, Z. Chang and X.-H. Bu. *ACS Appl. Mater. Interfaces*, 2019, **11**, 20995-21003.

14) He, Z. Zhang, S. Xiang, F.R. Fronczek, R. Krishna and B. Chen. *Chem. Commun*., 2012, **48**, 6493-6495.

15) H. Lyu, J. Zhu, B. Zhou, H. Cao, J. Duan, L. Chen, W. Jin and Q. Xu. *Carbon*, 2018, **139**, 740-749.

16) Z. Zhang, Q. Ding, J. Cui, X. Cui and H. Xing. Small, 2020, **16**, e2005360.

17) X. H. Han, K. Gong and X. Huang, J. Yang, X. Feng, J. Xie and B. Wang. Angew. Chem. Int. Ed., 2022, **61**, e202202912.

18) Y. Chen, Y. Yang, Y. Wang, Q. Xiong, J. Yang, S. Xiang, L. Li, J. Li, Z. Zhang and B. Chen. J Am. Chem. Soc., 2022, **144**, 17033-17040.